Dynamics of Turtle Horizontal Cell Response

RICHARD L. CHAPPELL, KEN-ICHI NAKA, and MASANORI SAKURANAGA

From the National Institute for Basic Biology, Okazaki, Japan 444

ABSTRACT The small- and large-field (cone) horizontal cells produce similar dynamic responses to a stimulus whose mean luminance is modulated by a white-noise signal. Nonlinear components increase with an increase in the mean luminance and may produce a mean square error (MSE) of up to 15%. Increases in the mean luminance of the field stimulus bring about three major changes: (*a*) the incremental sensitivity defined by the amplitude of the kernels decreases in a Weber-Fechner fashion; (*b*) the waveforms of the kernels are transformed from monophasic (integrating) to biphasic (differentiating); (*c*) the peak response time of the kernels becomes shorter and the cells respond to much higher-frequency inputs. The dynamics of the horizontal cell response also depend on the area of the retina stimulated. Smaller spots of light produce monophasic kernels of a longer peak response time. The presence of a steady background produces three major changes in the spot kernels: (*a*) the kernel's amplitude becomes larger (incremental sensitivity increases); (*b*) the peak response times become shorter; (*c*) the waveform of the kernels changes in a fashion similar to that observed with an increase in the mean luminance of the field stimulus. A similar enhancement in the incremental sensitivity by a steady background has also been observed in catfish, which shows that this phenomenon is a common feature of the horizontal cells in the lower vertebrate retina.

INTRODUCTION

The step-evoked response from turtle horizontal cells is composed of an initial peak followed by a plateau. The peak is produced by a sudden change in luminance and the plateau is maintained as long as illumination is maintained. The visual environs a turtle encounters in nature are a modulation of luminance around a mean, and turtle visual cells, including the horizontal cells, must be capable of responding optimally to such stimuli.

Several recent studies have described turtle horizontal cell responses in the presence of steady luminance. For example, Tranchina (1981) and Tranchina et al. (1983) used a sinusoidally modulated input, whereas Naka et al. (1982) made preliminary experiments with a white-noise–modulated input. Both groups came

Address reprint requests to Dr. Richard L. Chappell, Hunter College and City University of New York Graduate School, 695 Park Ave., New York, NY 10021. Dr. Sakuranaga's present address is Dept. of Physiology, Nippon Medical School, Bunkyo-ku, Tokyo, Japan 113.

J. GEN. PHYSIOL. © The Rockefeller University Press · 0022-1295/85/09/0423/31$1.00

Volume 86 September 1985 423–453

to the conclusion that turtle horizontal cells respond linearly to the large-field stimuli used. In this paper, we will elaborate on the horizontal cell response evoked by white-noise stimuli. Our conclusions are (*a*) that both small- and large-field turtle horizontal cells produce responses that can be predicted by the first-order kernels with mean square errors (MSEs) of <15%, and at some mean luminance levels (~0.5 $\mu W/cm^2$), the MSE can be <5%; (*b*) that the responses have different dynamics depending upon the mean luminance and the size of the area illuminated; and (*c*) that response dynamics can be modified by a steady surround illumination.

MATERIALS AND METHODS

Experiments were performed on the eyecup preparation of the red-eared turtle, *Pseudemys scripta elegans*, imported from the United States and kept in a tank at the National Institute for Basic Biology, Okazaki, Japan. After the turtles were decapitated, the eyes were enucleated and hemisected. Preparations kept at 20°C were placed in a chamber to which moist oxygen was continuously supplied. Recordings were made with microelectrodes filled with 2 M potassium citrate. The impaled cells were not identified morphologically but the cells' receptive field profiles were measured with a traveling random grating (Davis and Naka, 1980). We found that the response characteristics described in this paper were shared by the two types of luminosity horizontal cell responses: the small-field (L2) horizontal cell response, which has been identified with the horizontal cell soma, and the large-field (L1) horizontal cell response, which has been identified with the axon terminal (Simon, 1973; Leeper, 1978). The half-widths of the receptive field profiles obtained by cross-correlating the response to the traveling grating were 0.2–0.4 and 0.5–0.7 mm for the small- and large-field responses, respectively. Although we observed variations in the size of the field, the two parts of the cell could always be identified without difficulty by computing the size of the fields. Especially when responses were recorded simultaneously from the two parts located in close proximity (~0.4 mm) or when two recordings were made successively from a single penetration, the "busyness" of the response to a traveling grating easily allowed us to determine the part of a cell without computation (see Fig. 5*C*). The frequency response characteristics showed that the responses were cone-driven.

An amplifier (701, W-P Instruments, Inc., New Haven, CT) was used to match the impedance of the electrode with the main amplifier. The photostimulus was provided with a glow modulator tube (R-1130B, Sylvania/GTE, Exeter, NH) whose plate current was modulated either by a step input or by a white-noise signal with a power spectrum that was flat from near DC to 80 Hz. The white-noise signal was obtained from a white-noise generator (WG-772, NF Circuit Design Block, Tokyo, Japan). The signal source had an approximately Gaussian distribution with a peak-to-peak excursion of about eight times the standard deviation. The depth of modulation defined in the conventional fashion, $(L_{max} - L_{min})/(L_{max} + L_{min})$, was ~0.5–1 at 0 dB. In the experiment shown in Fig. 9, the depth of modulation of 0.5 (i.e., 50%) was reduced by −10 and −20 dB, which produced a depth of modulation of 16 and 5%, respectively. The depth of modulation of the white-noise signal is an approximation because of the statistical nature of the input. The mean luminance level was attenuated by interposing neutral density filters between the glow tube and the preparation. The stimulus had three spatial configurations: a spot of light with various diameters, the extremely large spot being referred to as a field, and a spot of light with a steady annular illumination (0.1–10 $\mu W/cm^2$). The smallest spot was 0.7 and the largest spot, the field, was 4.7 mm in diameter. The annular light had an

inner diameter of 0.74 mm. The mean luminance of the unattenuated (log $I = 0$) white-noise–modulated light was 50 $\mu W/cm^2$ at the retina. The range of mean luminance we used most of the time (much $>10^3$ photoisomerizations per rod per second at 500 nm) was high enough to saturate rod systems. Although the results described in this paper were all obtained without any chromatic filter, responses were confirmed as luminosity types using a light stimulus with a red filter (R-62, Hoya Corp., Tokyo, Japan, cutoff at 640 nm, 12 $\mu W/cm^2$).

Fig. 1 is a schematic representation of the system for measuring the light (input) and response (output). A photodiode (750, United Detector Technology, Culver City, CA) monitored the output from the glow tube before the light was attenuated by neutral

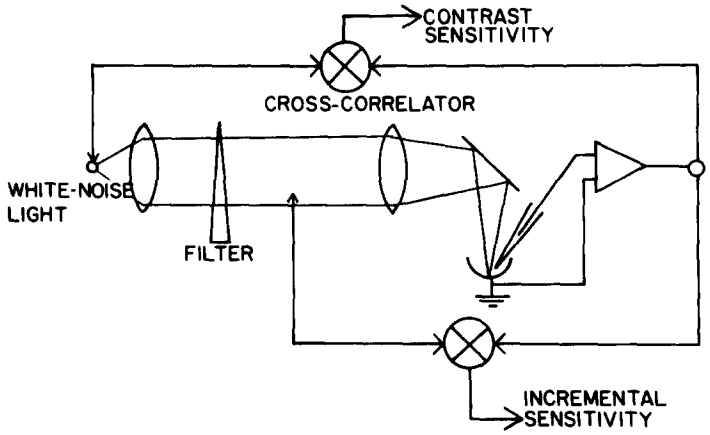

FIGURE 1. Scheme of procedure for measuring the light stimulus and the resulting response. The light stimulus was monitored by a photodiode before the signal was attenuated by a series of neutral density filters. A correlation was made between the unattenuated light signal and the response. The kernel computed was the contrast sensitivity because contrast of the light stimulus was kept unchanged although the absolute amplitude of the stimulus, both the mean and modulation, spanned a range of several log units. Incremental sensitivity can be obtained if a correlation is made between the stimulus after attenuation and the response.

density filters. Kernels were computed by cross-correlating the photodiode signal with the response. The kernels computed in this fashion are the contrast sensitivity at a given mean luminance, which is controlled by the filters. (Interposed filters changed the mean luminance, keeping the "depth of modulation" unchanged.) If the light signal is measured after attenuation, a correlation with the response will produce the incremental sensitivity. The direct measurement of the incremental sensitivity is not practical because of the limitations of the photodetector. (This retina is a better instrument than a man-made photodiode.) The contrast sensitivity, however, can be easily converted into the incremental sensitivity, as we will describe in Appendix A.

Data, both the input signal before attenuation and the horizontal cell response, were stored on analog tape (NFR 3000 data recorder, Sony Corp., Tokyo, Japan) and were digitized off-line at 500 Hz/s to be stored on the disk memory of a VAX 11/780 computer (Digital Equipment Corp., Marlboro, MA). Digitized data were first filtered at 0.1–100 Hz for light and 0.1–50 Hz for response signals, and a cross-correlation was made between the (unattenuated) light signal and the response.

For control experiments, we used channel catfish, *Ictalurus punctatus*, obtained locally. Turtle and catfish experiments were performed under identical conditions. For perfusion experiments, we used turtle Ringer (Cervetto and MacNichol, 1972) for both turtle and catfish experiments, except that, for catfish, bicarbonate was increased to 47 mM from the amount used by Cervetto and MacNichol. Ringer was constantly perfused and perfusion did not have any apparent effects on the step-evoked response or on the waveform and amplitude of kernels from the turtle horizontal cells. Bicuculline methochloride (Pierce Chemical Co., Rockford, IL) was dissolved directly in these saline solutions when it was used.

Algorithms for computation can be found in Sakuranaga and Naka (1985).

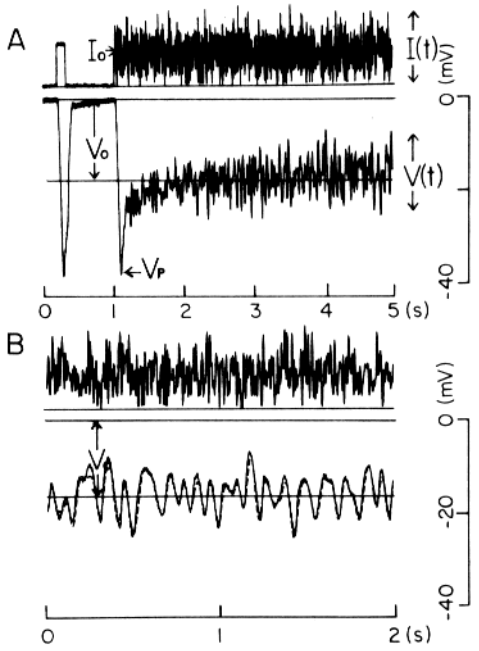

FIGURE 2. Time records of the responses from a turtle horizontal cell produced either by a step or white-noise–modulated stimulus. *A* shows the initial part of the white-noise–evoked response and *B* shows a part of the record after the response reached a steady state. The cell's dark potential level was referenced as 0 mV and I was 50 $\mu W/cm^2$. In *B*, the continuous line shows the cell's response and the dashed line gives the prediction by the first-order kernel. The prediction, with an MSE of 8.6%, was for the linear part of the response. See text for symbols.

THEORY

In their natural environs, turtle retinas receive light stimuli that are composed of two components, a steady mean (DC) with superimposed temporal fluctuations (AC). In most previous electrophysiological experiments, responses were evoked by a flash or a step of light given in the dark, as shown in the early part of Fig. 2*A*. In turtle horizontal cells, the responses evoked by such stimuli are composed of an initial hyperpolarizing peak, V_P, which settles down to a plateau, V_0 (Fig. 2*A*): a large sudden change in luminance produces nonstationary effects. In the response shown in Fig. 2, it took 3–4 s to reach a steady level. The transient response, the early part of the response evoked by a white-noise

stimulus in Fig. 2*A*, is not dealt with in this paper, and all analyses were made of the recordings where the DC component settled down to a steady level, as in Fig. 2*B*. The dynamics of the visual system, including horizontal cells, change with the mean luminance level (complete darkness is only a special case of the zero mean level). In this paper, we will analyze these changes in the response dynamics at different levels of mean (adapting) levels of luminance.

The Gaussian white-noise stimulus, $L(t)$, has two components, the mean luminance, I_0, and the time-varying modulation, $I(t)$, as shown in Fig. 2:

$$L(t) = I_0 + I(t). \tag{1}$$

The steady state horizontal cell response is composed of two components, the steady hyperpolarization, V_0, which is produced by I_0, and the time-varying part, $v(t)$, produced by $I(t)$:

$$V(t) = V_0(I_0) + v(t). \tag{2a}$$

In linear or quasilinear systems such as cones and horizontal cells, $v(t)$ can be expressed by the well-known convolution integral:

$$v(t) = \int_0^\infty h(\tau; I_0)I(t - \tau)d\tau, \tag{2b}$$

where $h(\tau; I_0)$ is the first-order kernel and $I(t)$ is an arbitrary stimulus. The first-order kernel $h(\tau; I_0)$ is obtained by cross-correlating the stimulus, i.e., the Gaussian white-noise modulation of $I(t)$, with the response. In Fig. 2*B*, the continuous line was a turtle horizontal cell's response to white-noise stimulus and the dashed line was the prediction computed by Eq. 2*b*. The cross-correlation process extracts the linear component from a response and enables us to estimate the degree of linearity of the response. The match between the two traces, observed (continuous line) and predicted (dashed line), in Fig. 2*B* was good but not perfect. A deviation of one from the other was observed occasionally. This was due to two factors: (*a*) noise present in the stimulus (input) and/or in the cell's response (output), or (*b*) the presence of nonlinear components.

The first-order kernel is, therefore, a cell's response (or the best linear approximation thereof) to a brief flash of light superposed on a steady mean luminance. This is shown in Fig. 3, where a cell's single response to a flash of light given on top of a steady illumination is superposed on the first-order kernel obtained with a white-noise stimulus whose mean was identical to that of the steady illumination. Although the flash response was noisy, the two traces produced a good match. The degree of deviation from linearity is measured in terms of the deviation between a cell's response (solid line), $V(t)$, and the linear component, $v(t)$, predicted by the first-order kernel (dashed line) in Fig. 2*B*:

$$\int_0^\infty [V(t) - V_0(I_0) - v(t)]^2 dt. \tag{3}$$

The mean square error (MSE) between the response and the prediction is given as a percentage by computing the ratio of the deviation defined by Eq. 3 to that for the case $v(t) = 0$. In the case of the response in Fig. 2*B*, the MSE was 8.6%. A significant MSE does not necessarily mean the actual discrepancies of the system point by point are that large because there are three reasons for a large MSE: (*a*) intrinsic noise in the membrane potential, (*b*) dynamic nonlinearity, and (*c*) the stochastic character of response. Responses of a smaller amplitude tend to produce a larger MSE because of intrinsic as well as extrinsic noises (which are unrelated to the stimulus). The −20-dB record in Fig. 9 had a large MSE of 15.7%, which was due to the small response amplitude. Another simple

criterion for assessing the degree of linearity in the input-output relationship is the probability density function (PDF) of the response to a Gaussian white-noise stimulus. If a response is linear, its PDF should also be Gaussian, as shown in Figs. 8 and 9*D*. The PDF of both input and output can be estimated by computing their amplitude histograms:

$$p(x) = \frac{N_x}{N\Delta x}, \tag{4}$$

where N is the total number of data points sampled and N_x is the number of data points falling within the narrow range $x \pm \Delta x/2$, with an interval Δx. The skewness appearing in a PDF is a simple measure of nonlinearity: conversely, if the PDF (of a response produced by white-noise input) is Gaussian, the response is possibly linear (McKean, 1973) and should be confirmed from the MSE in Eq. 3.

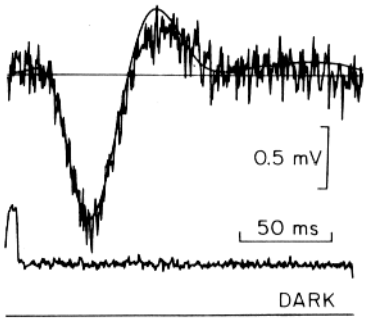

FIGURE 3. Comparison of a first-order kernel with a response evoked by a 5-ms flash of light, which approximated an impulse input, superposed on a steady luminance of 5 μW/cm^2. The white-noise stimulus used to measure the kernel had a mean luminance of 5 μW/cm^2. Although the pulse response was noisy, it can still be seen that after correction for a small constant drift, the kernel and the response matched well in their waveforms. The voltage scale applies only to the impulse response. The upper traces are the response and kernel. The lower trace is for the light stimulus.

RESULTS

The basic experimental scheme used in this paper is shown in Fig. 4. On the left are responses evoked by a series of steps of light given in the dark as their magnitude was increased by 1-log units. The 0.3-s flash produced only the initial transient peaks (V_P in Fig. 2), whose amplitude increased monotonically as the magnitude of step inputs was increased. If the stimulus was longer in duration or was white-noise–modulated, the initial transients settled down to the steady levels that are indicated by the dashed lines in the figure. (The levels were measured from the responses evoked by the white-noise stimulus.) On the right of the figure are the PDFs (labeled "amplitude histogram") of the responses evoked by white-noise stimuli whose mean luminances correspond to the full intensity of the step stimuli indicated. PDFs represented the dynamic modulation of the horizontal cell's response to a white-noise stimulus around the steady potential levels (V_0 in Fig. 2), as indicated by the dashed lines. PDFs were approximately Gaussian, although those obtained with 0- and −1-log stimuli

were slightly skewed, which indicated that, with stimuli of higher mean luminance, nonlinearity appeared. As we will describe later, nonlinearity was of compression type and the nonlinear component was <15% in an MSE sense. Note, however, that the response excursions as indicated by PDFs covered a large range that was nearly 30 mV peak to peak for the −1-log record. This was a piecewise linearization of the response around a steady mean level, V_0. In the description that follows, we will substantiate this finding.

The records in Fig. 5 were obtained simultaneously from a small- (L2) and a large- (L1) field horizontal cell. The responses were evoked by temporally

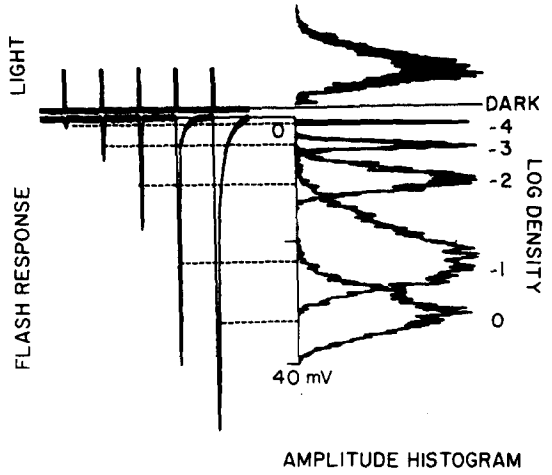

FIGURE 4. Comparison of step-evoked responses with those produced by a white-noise stimulus. The step-evoked responses were for the (initial) transient part of a cell's response, whereas white-noise–evoked responses were the cell's response to perturbation around a mean luminance after the cell's response reached a steady state. The light stimulus was measured before it was attenuated by neutral density filters. The dashed lines were measured from white-noise–evoked responses and show the steady state levels of hyperpolarization. Log density indicates the value of neutral density filters interposed. The amplitude histogram gives the PDF obtained at the corresponding steady state level.

modulated white-noise light (*A* and *B*) or by a traveling random grating (*C*). Records *A* and *B* were the initial and steady state responses to white-noise stimuli. The two cells produced identical temporal responses, as seen by the two superposed traces shown in *A* and *B*, one from the small-field cell and the other from the large-field cell. A random grating, on the other hand, produced very different responses in these cells: the small-field unit responded very vigorously (lower trace in *C*) and the large-field unit responded poorly (middle trace in *C*) to the traveling grating. Fig. 5*D* shows the correlograms from the grating experiment. As shown by Davis and Naka (1980), the correlograms are an approximation of the receptive field profiles: the dotted lines are for the small-field (half-width of 0.3 mm) unit and the continuous lines are for the large-field (half-width of 0.7 mm) unit. A similar observation was made in catfish in which the horizontal cell

soma (field half-width of ~0.5 mm) produced a vigorous response, whereas the horizontal cell axon (field half-width of >1 mm) produced a very weak response to the traveling grating (Sakuranaga and Naka, 1985).

Fig. 6 shows first-order kernels from a large- (solid lines) and a small- (dotted lines) field unit obtained with white-noise stimuli whose mean luminances covered

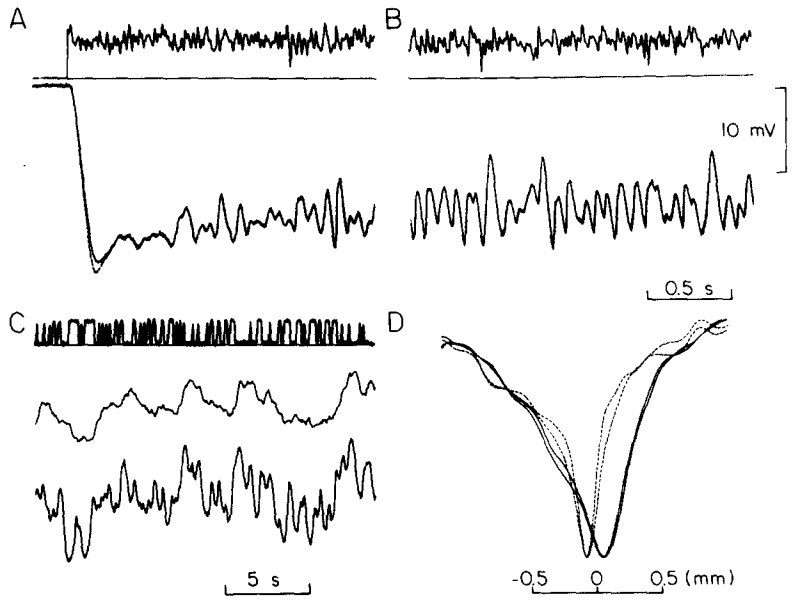

FIGURE 5. Responses recorded simultaneously from a small- (L2) and a large- (L1) field horizontal cell. *A* and *B* are time records. *A* shows the cell's response when the white-noise stimulus was turned on and *B* shows the steady state responses. The upper trace is the light stimulus and the lower superposed traces are responses with a solid line for the L1 and a dotted line for the L2 cell. *C* shows the response of the cells to a traveling random grating. The upper trace is the intensity variation of traveling random grating monitored by a photodiode with a very narrow slit and the lower two traces are the L2 (middle trace) and the L1 (lower trace) responses. *D* shows the correlogram computed from the records of which a part is shown in *C*. The correlograms are the (approximated) profiles of the cells' receptive fields. The solid lines are for L1 and the dotted lines are for L2. The two superposed traces are from two different runs from the same pair. The distance between the two electrodes in the direction of grating movement is indicated by the distance between the two peaks since two electrodes were aligned diagonally to the grating.

3 log units. Fig. 6*A* shows kernels without scaling, where a correlation was made between the light signals before attenuation and the resulting response. The neutral density filters were −3, −2, −1, and 0 log density for the four pairs of records. The brighter stimulus produced faster kernels. The kernels, as they are plotted here, are the contrast sensitivity, $S_c(t)$, defined in Appendix A. The kernels obtained without any density filter are also the incremental sensitivity, $S_i(t)$. With a thousandfold increase in the mean intensity, the kernel's amplitude,

i.e., the contrast sensitivity, increased only by 10-fold (amplitudes were measured on the hyperpolarizing phase). With the two brighter mean luminances, the kernels had almost identical amplitudes: these two response amplitudes followed the Weber-Fechner function. In Fig. 6*B*, the kernels are normalized for a comparison of their waveforms. The kernels in Fig. 6 show that: (*a*) with an increase in the mean luminance, the waveform of the kernels changes from being integrating (monophasic) to differentiating (biphasic), which indicates that the cells were responding to the amplitude of the stimulus when the mean was low

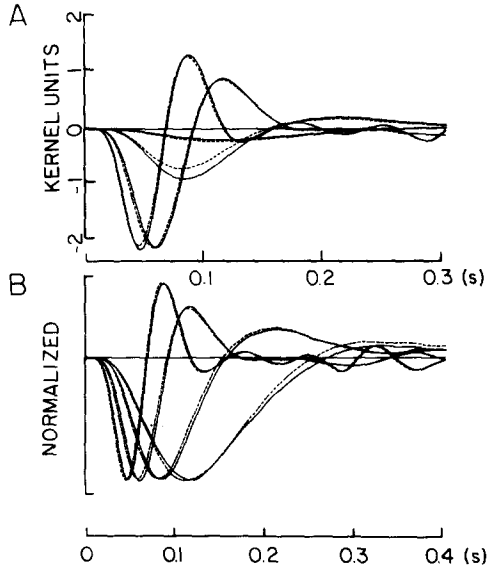

FIGURE 6. First-order kernels from L1 and L2 units measured at four mean luminance levels. The maximal mean luminance was 50 $\mu W/cm^2$ and was attenuated by 1 log steps. The solid lines are for L1 and the dotted lines are for L2 units. In *A*, kernels are the contrast sensitivity because they were computed by cross-correlating the light signal before attenuation with the response. The ordinate ($mV/\mu W/cm^2/s$) applies to the 0-log kernels (largest), which are also the incremental sensitivity. In *B*, kernels are normalized to compare their waveforms. Note that there are different time scales for *A* and *B*.

and to changes in the amplitude when the mean was high; (*b*) the peak response time became shorter and the width of the kernel became narrower with an increase in the mean luminance, and the cells responded to faster inputs (higher frequency) when the mean luminance was brighter; (*c*) the dynamics, both contrast sensitivity and waveforms of kernels, were almost identical for the two cells over a large range of mean luminances. This is what one would have expected from the time records shown in Fig. 5.

The dependence of the dynamic characteristics upon the mean luminance level did not differ from experiment to experiment. Fig. 7 shows the response dynamics measured from four large-field units at four mean luminance levels. The mean of the unattenuated 0-log illumination differed from cell to cell, while

the dynamic change with mean luminance level characterized by the waveform of first-order kernels was almost identical for four cells over the 3-log range of mean luminances. The amplitudes of responses from these four cells were also computed as functions of frequency of input modulation from the first-order

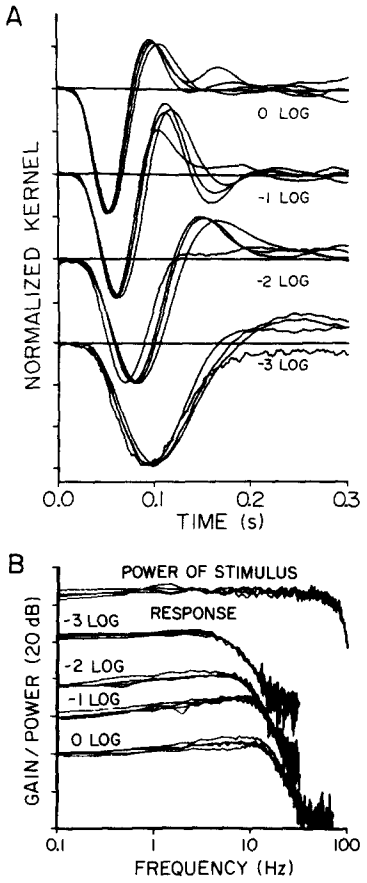

FIGURE 7. First-order kernels and gain functions from four L1 units measured at four mean luminance levels. In *A*, superposed kernels are normalized and shifted by an arbitrary step according to 1 log attenuation of mean luminance level. The unattenuated mean luminance of 0 log for each unit differs from cell to cell, while the dynamic change with mean luminance is similar for these four units. In *B*, gain functions (amplitude parts of transfer function) are arbitrarily shifted without changing the dependence upon mean luminance level. Four power spectra of light stimuli are also superposed.

kernels using a fast Fourier transform (FFT) algorithm; the result is shown in decibels in Fig. 7*B*. The amplitude of the responses decreased by ~20 dB and the cutoff frequency increased from ~2 to ~10 Hz with an increase in the mean luminance level. Gentle peaks appeared around the cutoff frequency for higher mean luminance, which reflects the biphasic character of first-order kernels at higher mean luminance.

Fig. 8*A* shows the time records of the light input (upper trace) and the resulting horizontal cell response in a white-noise experiment, together with the (amplitude) PDF of each. In the response trace, the continuous line is the cell's actual response and the dotted line is the model response predicted by the first-order kernel based on Eq. 2*b*. Note that the two time traces, one for the response and

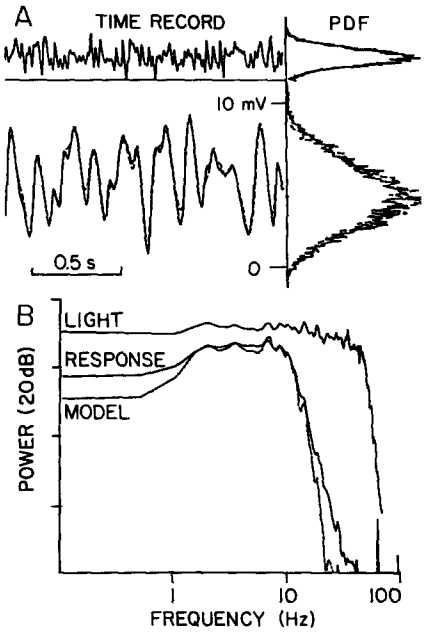

FIGURE 8. (*A*) Time records of light stimulus (upper trace) and responses (lower trace) with their PDFs. In the response record, the solid line is the cell's response and the dotted line the prediction (model) by the first-order kernel. Both the response time record and the PDF are closely matched by the predicted ones. (*B*) Power spectra of stimulus, response, and prediction. The power spectrum of the predicted response deviates from that of the cell's response in the lower- and higher-frequency range. The deviation in the lower range was due to the short recording time (40 s) and the deviation in the high-frequency range was due to the nonlinear components. The MSE of the predicted response was 7.6%.

the other for the linear model, superimpose upon each other, as do the two PDFs observed from them. The response is quite linear and the MSE calculated for this particular record was 7.6%. This linear response was obtained over a potential excursion of >10 mV. The power spectra for the light input and the actual and predicted responses (from the first-order kernel) are shown in Fig. 8*B*. Except for the two extreme frequency ranges, low and high, the response and model power spectra are almost identical, which confirms our observations made in the time record.

We have consistently observed that the turtle horizontal cell's response evoked by white-noise–modulated field illumination is linear, with MSEs usually <15% over a large range of mean luminance (up to 80 $\mu W/cm^2$). Furthermore, this

linearity held over a large range of modulation (while the mean was kept unchanged). This is shown in Fig. 9, where the depth of modulation of the white-noise signal was decreased from 0 to −20 dB (the mean luminance was held constant). Fig. 9, *A* and *B*, shows parts of the same record; *A* is the initial segment and *B* is the steady state record, during which the depth of modulation was

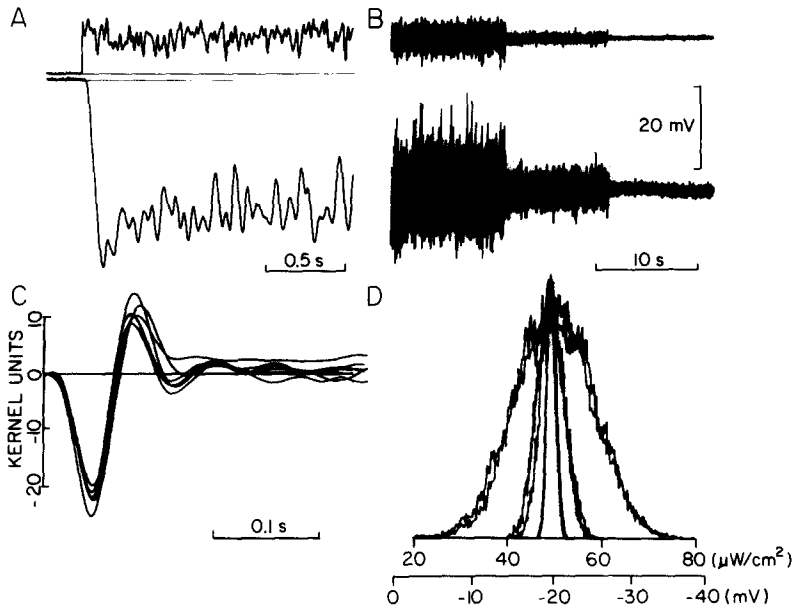

FIGURE 9. Responses evoked by white-noise stimuli of different powers. (*A*) Initial part of the white-noise input (upper trace) at 0 dB and evoked response (lower trace). (*B*) The responses (lower trace) evoked by white-noise stimuli (upper trace) of 0, −10, and −20 dB in power. (*C*) Six kernels obtained from two cells with white-noise stimuli of 0, −10, and −20 dB. Although the power is different for each stimulus, the kernels are similar in their amplitude as well as in their waveforms. The ordinate units are in mV/μW/cm²/s. (*D*) PDFs of light and responses, scaled so that the light and response PDFs matched. The PDFs of both stimulus and response are superposed for 0, −10, and −20 dB inputs. The voltage scale is from the dark level of the horizontal cell membrane potential. In all other figures in this paper, the depth of modulation was kept constant, with the mean luminance changed by interposing a series of neutral density filters as shown in Fig. 1.

changed by 10-dB steps. Note that the mean hyperpolarization remained unchanged, but the amplitudes of the voltage fluctuation produced by the white-noise signal decreased roughly in proportion to the decrease in the input signal. Fig. 9*C* shows kernels from 0-, −10-, and −20-dB white-noise signals (six kernels from two cells are shown). The kernels were similar in their amplitude as well as in their waveform for the three white-noise signals (0, −10, and −20 dB): the incremental sensitivity and dynamics remained unchanged, which is what we would expect from a linear system. This observation is confirmed by the PDFs in *D*, where three pairs of two superposed traces, one for the light stimulus and

the other for the horizontal cell response, are superposed by the scaling of light and potential axes. As we noted in *B*, the PDFs for light and response changed in proportion to the degree of modulation, which indicates that the response was linear. The MSEs were 10.6% for 0 dB, 3.8% for −10 dB, and 15.7% for −20 dB. Note that the voltage excursion for the 0-dB record was nearly 40 mV. The large MSE for the −20-dB record was due to the small response signals and the large MSE for the 0-dB record was due to the appearance of complex nonlinear components (see Fig. 11).

Although the response could be predicted by the first-order kernels with MSEs of <15%, we have observed a consistent deviation of the response from linearity for various mean luminances, as illustrated in Fig. 10. This figure shows MSEs from experiments in which responses were recorded simultaneously from the

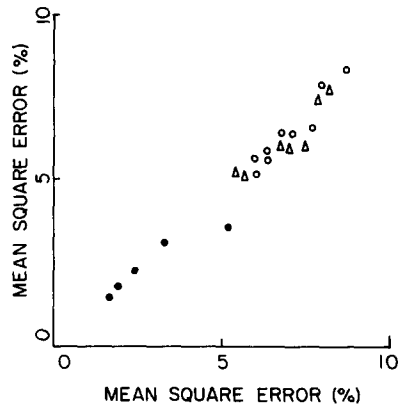

FIGURE 10. MSEs of the predicted model (by the first-order kernel). Data are from experiments in which two horizontal cell responses were recorded simultaneously. The cells of each pair, which produced larger MSEs, are plotted on the abscissa and those that produced smaller MSEs are plotted on the ordinate. Open circles are for 0 log, traingles for 1 log, and closed circles for 2 log attenuation.

two horizontal cells at three mean luminances, 0.8, 8, and 80 $\mu W/cm^2$, having the same depths of modulation. The larger of the two MSEs is plotted on the abscissa. The pairs of records whose MSEs were <10% were tabulated. The points fell on the diagonal, which indicates that the responses recorded simultaneously from two cells produced almost identical MSEs (under good recording conditions). The MSEs for low luminance inputs were much smaller than the MSEs for higher mean inputs. The inputs of much lower mean luminance (not plotted) produced larger MSEs (>10%) because of the small response amplitude and the poor signal-to-noise ratio. In general, once the signal-to-noise ratio was no longer a factor, increasing the mean luminance introduced more nonlinearity into the response.

The dynamic nonlinearity seen in the responses evoked by stimuli of high mean luminance was the compression (second-order) nonlinearity, which is a reflection of the static nonlinearity (Naka-Rushton relationship). The second-order nonlinearity is (as an approximation) produced by an interaction of two

pulses. A second-order kernel, therefore, is a three-dimensional solid with two times axes, tau 1 and tau 2, which represent the time relationship of two pulses. In a two-dimensional plot, as shown in Fig. 11, the magnitude of nonlinearity, the third dimension, is shown by the contour lines. The nonlinearity produced by two pulses given simultaneously appears on the diagonal of the kernel; this

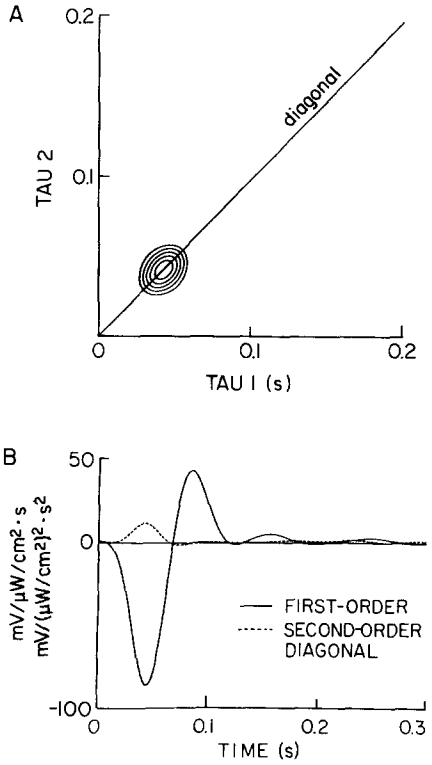

FIGURE 11. Typical second-order kernel from a turtle horizontal cell. A second-order kernel is a three-dimensional solid with two times axes, tau 1 and tau 2, and the third axis indicates the magnitude (contour lines) of the nonlinear kernel. The second-order kernel had a solitary depolarizing peak on the diagonal to indicate that two pulses of light given simultaneously produced a depolarizing nonlinear response. The nonlinearity was therefore produced by an increase in the stimulus amplitude. In the lower figure, the diagonal cut of the second-order kernel is shown by the dashed line. It is a side view of the kernel. The figure also shows the first-order kernel from the same cell (solid line). Note that the hyperpolarizing linear response was opposed by the depolarizing nonlinear response but not the after-depolarization in the linear response. By this intricate time relationship, the nonlinear response produced the compression (or rectification) of the large hyperpolarizing respone without interfering with the depolarizing phase of the linear response. The ordinate units in the lower figure (in $mV/\mu W/cm^2/s$) are for the first-order kernel only.

nonlinearity produces a deviation of the dynamic response from the law of amplitude-wise superposition. One example of the second-order kernel from a horizontal cell is shown in Fig. 11. The nonlinearity appeared as a single depolarizing peak, which was on the diagonal line. In Fig. 11*B*, the diagonal cut, the side view of the second-order kernel, is also shown, (dashed line), together with the first-order kernel (solid line) computed from the same response. As the nonlinear peak was on the diagonal line, the first-order kernel and the diagonal cut of the second-order kernel were the linear and the nonlinear part of the cell's response to a brief flash of light superposed on a mean luminance. The waveform of the diagonal cut was the mirror image of the initial negative phase of the first-order kernel. The hyperpolarization produced by the first-order kernel was opposed by the depolarization produced by the second-order kernel; this is a compression nonlinearity. The amplitude of the linear part of an impulse response, as indicated by the first-order kernel, is linearly related to the amplitude of the input, whereas that of the nonlinear component is a quadratic function of the input: the larger the input was, the larger was the depolarization produced by the nonlinear component. The diagonal cut was monophasic, whereas the first-order kernel was biphasic. The depolarization produced by the after-depolarization of the first-order kernel was not opposed by the second-order kernel. This intricate time relationship between the first- and second-order kernels enhanced the band-pass (transient) characteristics of the response observed at high mean luminance levels.

The (first-order) kernels, as measured in this paper, are the contrast sensitivity, $S_c(t)$, of the cell at the mean of the white-noise stimulus. The incremental sensitivity, $S_i(t)$, can be obtained by dividing the contrast sensitivity by the value of the mean luminance. (This can be seen by comparing Eqs. 7 and 8 in Appendix A.) In Fig. 12*A*, we have plotted the value of contrast and incremental sensitivities obtained over a 4-log luminance range. Fig. 12*B* shows the peak response time of the kernels. The contrast sensitivity (filled circles plotted on a linear scale) increased with increase in the mean luminance. The incremental sensitivity (×'s plotted on a log-log scale) was Weber-Fechner-like for brighter mean luminances, but leveled off for low mean luminances. These data can be fitted with the modified Weber-Fechner relationship, in which the dark light is introduced (Fechner, 1860, and see Eq. 12 in Appendix A). The peak response times also became shorter as the mean luminance was increased (see Fig. 6). The MSE of the peak response time for brighter mean luminance was very small, which indicates that the turtle horizontal cells produced stereotypical responses. Simultaneous recordings from two horizontal cells often produced responses or kernels that were almost identical in their time courses or waveforms. One such example is shown in Figs. 5 and 6.

So far we have described turtle horizontal cell responses evoked by a large field of light. The dynamics of the turtle horizontal cell response, as in the catfish (Marmarelis and Naka, 1973), were dependent upon the size of the area illuminated. This is shown in Fig. 13, in which responses obtained by spots of various diameters—0.7, 1.4, 2.8, and 4.8 (large field) mm—are marked 1–4. The step-evoked responses shown in Fig. 13*A* not only became larger as the area stimulated

was made larger, but the waveforms of the response also changed. The response evoked by a small spot of light had slower on and off phases, whereas a larger spot produced a response with an initial peak and a faster return toward the dark level. A hump also appeared on the depolarizing phase: an increase in the

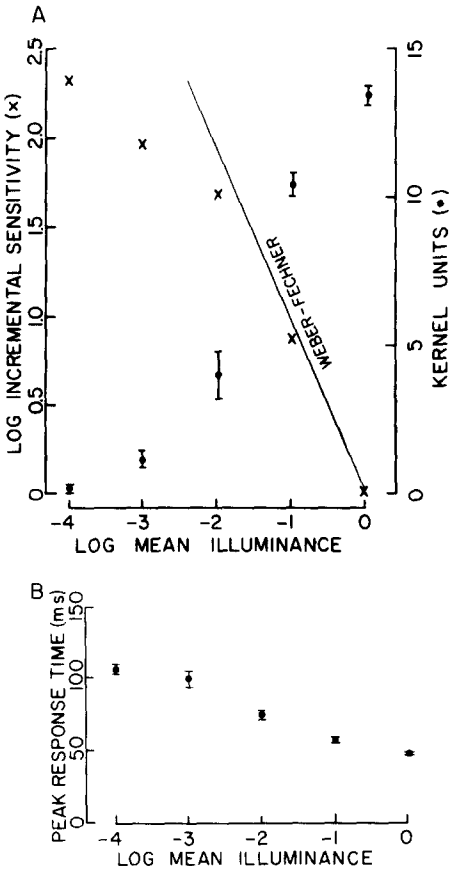

FIGURE 12. (*A*) Contrast and incremental sensitivity at five mean luminance levels. The right ordinate is for the contrast sensitivity. With no neutral density filter (0 log), the ordinate is also the incremental sensitivity and the kernel unit is in mV/μW/cm^2/s. The left ordinate is for log incremental sensitivity. The MSE is shown for the contrast sensitivity. From seven units. (*B*) Mean peak response times at four mean luminance levels with the MSE. From seven units.

area not only increased the response amplitude, but also changed the response dynamics. Fig. 13*B* shows the first-order kernels from the same cell shown in *A*. The kernel was integrating (monophasic) for a small spot of light and became differentiating (biphasic) for large spots of light (Fig. 13*C*). The small spot of light produced a smaller and slower response, whereas the larger spots produced larger and faster responses. These changes in the kernel waveforms are somewhat similar to the changes observed with an increase in the mean luminance observed in Fig. 6.

The slow response to a small spot of light could be made larger and faster by imposing a steady annular illumination. The responses in Fig. 14 were evoked by a spot (diameter, 0.7 mm), a spot of light with a steady annular illumination, and a field of light (for traces *A*, *B*, and *C*, respectively). The step-evoked spot response (*A*) had slow on and off phases (as observed in Fig. 13) and the response to a white-noise stimulus was sluggish. The same spot stimulus (*B*), in the presence of a steady annular illumination, produced a smaller but faster step response and

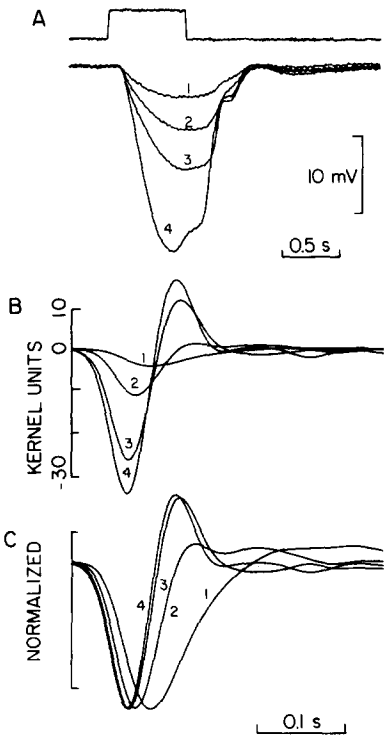

FIGURE 13. Responses evoked by spots of various diameters from an L2 unit. In *A*, the responses were evoked by step, and in *B* and *C* by white-noise modulation. In *B*, the ordinate is in $mV/\mu W/cm^2/s$, and in *C*, kernels are normalized. Spot diameters were 0.7, 1.4, 2.8, and 4.8 (large field) mm for traces 1–4, respectively. The mean luminance was 80 $\mu W/cm^2$.

a larger white-noise response. Note the membrane potential displacement by the steady illumination. The steady background produced a steady hyperpolarization of 17 mV from the dark level indicated by a line. Kernels computed from the data are shown in Fig. 15*A*. The small monophasic spot kernel (S) became larger as well as differentiating with annular illumination (S/A). When normalized, this spot/annulus kernel (dashed line) matched exactly the field kernel (F), except that the two superposed traces were separated after 0.1 s. In Fig. 15*B*, the power spectra of the responses are shown together with those predicted by the first-order kernel: the predicted spectra always lacked the faster components. The power spectrum of the spot-evoked response was a constant-gain low-pass with a

corner frequency of a few hertz (S). The steady background transformed the power spectrum from low-pass to band-pass with a corner frequency of ~10 Hz (S/A). Note also the much steeper roll-off of the power spectrum with a steady background. The power spectrum of the field-evoked response (F) had much greater power but the response characteristics were similar to those seen in the spot spectrum with a steady background. We noted that the increase in the

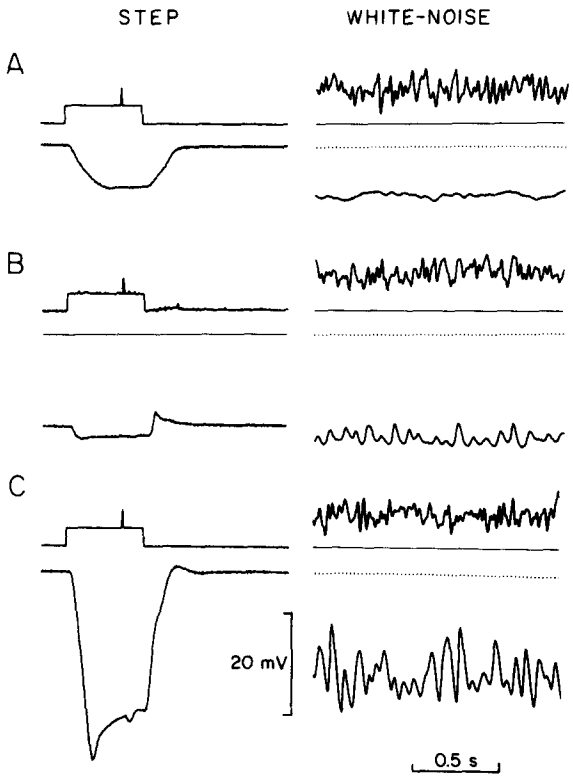

FIGURE 14. Step- and white-noise–evoked responses by a spot (*A*), a spot with a steady annular (0.74 mm i.d.) illumination (*B*), and a field of light (*C*). The step of light had a brief increment superposed. In *B*, the steady illumination displaced the membrane potential by 15 mV. Note that the spot-evoked response had a slower on and off phase, whereas the same spot of light produced a faster but smaller response in the presence of a steady annular illumination.

incremental sensitivity by a steady annular surround was mostly due to an improvement of the response in the high-frequency region of ~5–14 Hz. This is what one would expect from the faster and differentiating kernels in *A*. We always observed this enhancement of the spot response in both small- and large-field units. The degree of enhancement, however, was dependent upon the size and luminance of the spot stimulus, as well as the luminance of the steady surround (Kawasaki et al., 1984). Burkhardt (1974) reported a similar enhancement in the response to steady (1 s) spot illumination in some of the mudpuppy

horizontal cells recorded. Note here that the sustained response may actually decrease, whereas the dynamic increment response is substantially enhanced (Fig. 15 and compare Fig. 14, *A* and *B*).

Fig. 16*A* shows records from four L2 units. Recordings were made by a standard illumination pattern i.e., a white-noise–modulated spot of 0.7 mm diam

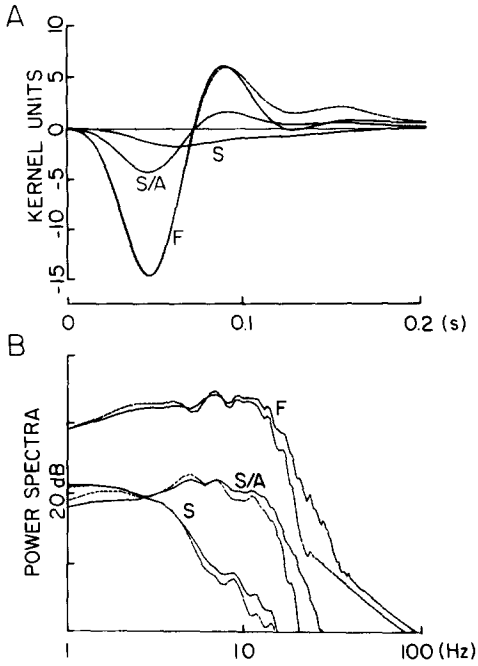

FIGURE 15. Kernels (*A*) and power spectra (*B*) computed from the experiments shown in Fig. 14. The spot produced a monophasic kernel that became biphasic in the presence of steady annular illumination. Superposed on the field-evoked kernel (the largest kernel) is the normalized spot kernel (dashed line) obtained in the presence of the steady illumination. These two traces match exactly from 0 to 0.1 s. In the power spectra, each pair of traces is for the measured response and for the model (dashed lines) predicted by the first-order kernel. The ordinate for *A* is in $mV/\mu W/cm^2/s$.

and a steady annulus of 0.74 mm i.d. The mean luminance was 0.5 $\mu W/cm^2$ for both inputs. The spot alone produced monophasic (integrating) kernels (S), with peak response times of ~100 ms. The presence of a steady annular illumination, as shown in Fig. 15, made the kernels (S/A) larger, faster, and biphasic (differentiating). In regard to amplitude, the sensitivity increased by a factor of 2. Fig. 16*B* shows results obtained from catfish horizontal cell somas. As in the turtle, the presence of steady annular illumination made the kernels larger, faster, and biphasic. The changes in catfish were even more drastic than in turtle, with steady annular illumination bringing about the same types of changes in the incremental sensitivity of its horizontal cells.

In catfish, bicuculline, a γ-aminobutyric acid (GABA) antagonist, transformed the horizontal cell kernels, presumably through interfering with the GABA-mediated synaptic transmission (Lam et al., 1978). In the presence of bicuculline, biphasic fast kernels became monophasic. The changes were the reverse of what we found in Figs. 14–16, where we found that the presence of steady annular illumination transformed kernels from monophasic to biphasic. In the experiments shown in Fig. 17, we examined the effects of bicuculline on turtle

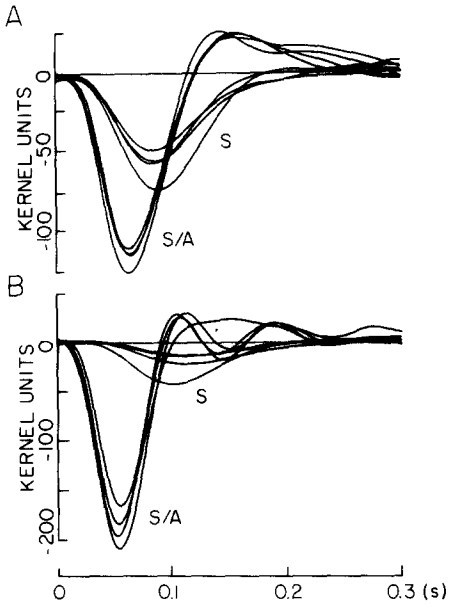

FIGURE 16. Steady annular illumination had similar effects on both turtle (*A*) and catfish (*B*) horizontal cells. Sets of kernels from four different horizontal cells are shown for each. The mean of the white-noise light on the spot was ~1 $\mu W/cm^2$. Kernel units are in $mV/\mu W/cm^2/s$ (the incremental sensitivity). Kernels marked S are for the spot alone and those marked S/A are for the same spot with a steady annular illumination. Note that (*a*) as the amplitude of the kernels became larger incremental sensitivity increased, (*b*) as the peak response time became shorter, the cell followed much faster signals, and (*c*) as the kernels became biphasic, the responses became differentiating.

horizontal cells. The figure also shows a result from catfish that served as a control. The stimulus used was a step with a superposed increment followed by a white-noise modulation with a mean of 1 $\mu W/cm^2$. The two superposed traces are the control trace (solid lines) and the trace made during perfusion with bicuculline Ringer (dotted lines). The amplitudes of the responses were adjusted so that the traces were superimposed. As indicated in the figure legend, the amplitude did not differ by more than 20% during the experiments. Perfusion was maintained from 5 to over 30 min and possible changes in response were continuously monitored. In spite of many attempts at perfusion with bicuculline

Ringer, we have not found any evidence to show that bicuculline had any effects on the temporal dynamics of turtle horizontal cells for doses ranging from 1 to 100 μM. The records shown in Fig. 16*A* are an example. In catfish, bicuculline produced very marked effects. The on phase became very slow and the increment failed to produce any response, which is what Lam et al. (1978) found. We have also examined the receptive field profiles with a traveling random grating. In turtle the field became smaller, but in catfish no change in the field profile was observed.

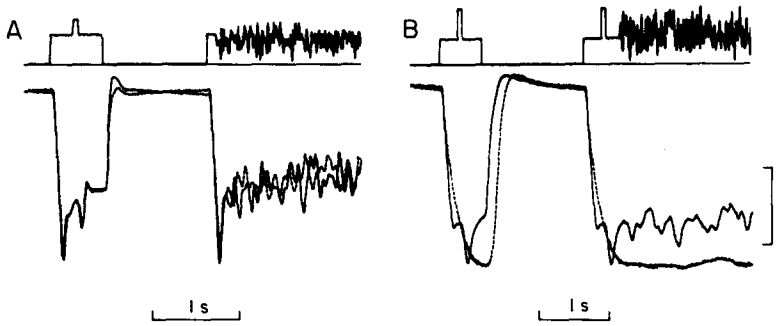

FIGURE 17. Bicuculline effects on responses from turtle (*A*) and catfish (*B*) horizontal cells to a step with increment followed by white-noise light stimulus. A higher concentration (50 μM) of bicuculline applied to the turtle retina caused negligible changes in its horizontal cell response compared with the effect at 10 μM bicuculline on the catfish horizontal cell. The vertical scale is 10 mV for the control Ringer (solid lines) responses and 12 and 8 mV, respectively, for the turtle and catfish in bicuculline (dashed line). Note that the time scaling differs.

DISCUSSION

This paper deals with changes in the incremental sensitivity and dynamics of turtle horizontal cells brought about by changes in the mean luminance, as well as with how the sensitivity and dynamics were influenced by spatial patterns of stimuli. The analysis performed here relates to the dynamics of the cell's response at a steady state; responses were evoked by modulation of a steady mean luminance, whereas most of the past analyses were made on the initial transient of step-evoked responses. It has long been known that the presence of a steady luminance influences the sensitivity of the visual system. Changes brought about by a steady illumination are the field (or light) adaptation, whose principal feature is the decrease in incremental sensitivity with brighter adapting (background) light. Classically, such a decrease is the Weber-Fechner relationship (Rushton, 1965). Field adaptation, as noted by Kelly (1971) in the human visual system and by us in turtle horizontal cells, is a very complex phenomenon of which one facet is a decrease in the incremental sensitivity.

To analyze such a complex phenomenon, we used white-noise–modulated light as a stimulus and applied the cross-correlation technique to determine the relationship between the stimulus and response, which is known as white-noise

analysis (Marmarelis and Naka, 1972). The methodology is appropriate for this study because: (*a*) the white-noise stimulus is designed to examine steady state but not transient dynamics, (*b*) cross-correlation is a time average to extract statistical measures as well as signals from noise (reliable measurements can be made over a large dynamic range), and (*c*) dynamics are systematically defined. The first-order kernels are the best linear approximation of a cell's response to a brief flash of light superposed on a steady luminance, which is the mean of white-noise stimulus. Similarly, the second-order kernels are the best approximation of the (second-order) nonlinear part of a cell's response to a brief flash of light superposed on a steady mean luminance (this is so because there was only the diagonal peak in the second-order kernels from turtle horizontal cells). The kernels, therefore, define the incremental sensitivity in a generalized sense (Appendix A) and allow us to segregate the linear and nonlinear components in the response.

There are three major findings in this paper: (*a*) changes in the response dynamics with changes in the mean luminance, (*b*) piecewise linearization of the response, and (*c*) the influence of spatial pattern on the incremental response.

As the mean luminance increased, we observed three changes in the first-order kernels: (*a*) their amplitude decreased roughly in a Weber-Fechner fashion, (*b*) their peak response times decreased, and (*c*) their waveform changed from monophasic to biphasic. Although the first observation is a well-known fact, its derivation is not so obvious. In catfish, the incremental sensitivity was not Weber-Fechner-like, but was the local slope of the Michaelis-Menten, or empirical Naka-Rushton, curve (Naka et al., 1979). In turtle, the absolute (DC) sensitivity of the luminosity-type horizontal cells was Michaelis-Menten-like (Fuortes et al., 1973), but the dynamic sensitivity was Weber-Fechner-like. The thesis, therefore, that the incremental sensitivity was the local slope of step-evoked responses did not hold. In Appendix A, we will present a formal explanation of the conversion of the incremental sensitivity of the Michaelis-Menten-like system to the Weber-Fechner function.

An increase in the mean luminance brought about a twofold change in the time course of the response dynamics: (*a*) brighter mean luminance made the response faster, as shown by the kernel's shorter peak response times (Fig. 12*B*), to show that the horizontal cells responded to inputs of faster temporal frequency; (*b*) the waveform of kernels was transformed from monophasic (integrating) to biphasic (differentiating), as shown in Fig. 6. In the frequency domain presentation, this corresponds to a transformation of power spectra from low-pass to band-pass. At lower mean luminance levels, the cells were responding more to the magnitude of stimulus, whereas at higher mean levels, the cells were responding more to the changes in the stimulus.

Over a large range of mean luminance (~4 log units), the horizontal cell response could be predicted by the first-order kernels with small MSEs of ~4% for the mean of 0.5 $\mu W/cm^2$, which became 7–15% as the mean luminance was increased. This linearity held for large voltage excursions, which in some cases exceeded 30 mV (Fig. 9*D*). The high degree of linearity held only for the responses evoked by a large field of light and for the responses from "good"

preparations, in which a step of light produced a response with a sharp initial transient. Responses evoked by a small spot of light or responses recorded from deteriorating preparations had a large degree of nonlinear component. One example is shown in Fig. 18, in which the luminance of a spot or a large field of light was modulated by a sinusoidal sweep. The response evoked by a small spot of light (Fig. 18*A*) had three features that were different from the response evoked by a large field of light: (*a*) the response was evoked only by the stimulus of low frequency, (*b*) the response waveform was sawtooth-shaped rather than sinusoidal, and (*c*) the response was rectifying. The stimulation of a large area somehow made the response faster, as shown in Fig. 12, and sinusoidal, which

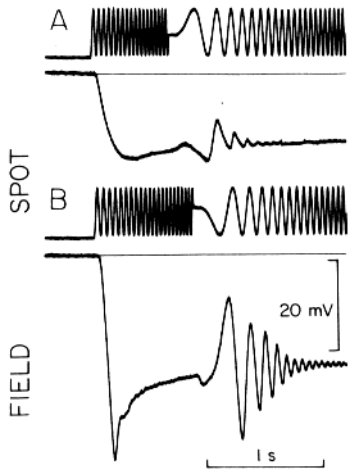

FIGURE 18. Responses from a turtle horizonal cell to a small spot (0.4 mm diam) and a large field of light whose luminances were modulated as sinusoidal sweeps. Note that the spot-evoked response lacked the initial transient produced by the mean of the stimulus. The large field of light produced responses that were (*a*) sinusoidal, (*b*) symmetrical around the mean hyperpolarization, and (*c*) of larger amplitude. A large field of light somehow linearized the incremental response.

suggests that stimulation of a large area produced some active changes that linearized the response.

A similar analysis of the temporal dynamics of turtle horizontal cells was reported by Tranchina (1981) and Tranchina et al. (1981, 1983, 1984). They used a sinusoidal stimulus, and impulse responses were obtained by the inverse Fourier transform from frequency domain data. As the turtle horizontal cells responded linearly to modulation around a mean luminance, the two approaches, sinusoidal and white-noise, should lead to the same results. Their conclusions were similar to ours in that (*a*) the harmonic distortion was very small, which indicates a small degree of nonlinearity, (*b*) the gain of low-frequency response was inversely proportional to the mean, which indicates a Weber-Fechner relationship, and (*c*) the waveform of impulse response changed from monophasic to biphasic. Kelly (1971) has computed impulse responses for the human visual

system from the analysis of flicker data, and the series of impulse responses for various mean luminances he obtained for humans bears a striking similarity to the series of kernels from the turtle horizontal cell. In both cases, the amplitude of the kernel (or impulse response) decreased with an increase in the mean luminance in an approximately Weber-Fechner fashion, and the impulse response, like turtle horizontal cell kernels, changed from integrating to differentiating as the mean luminance was increased. We have modified the model that was presented in Kelly's analysis, and we have obtained a more thorough agreement between the observed and modeled kernels, i.e., impulse responses (Appendix B). The revised model could show a similarity between turtle and human data, and could show that the change of dynamics according to the mean luminance was reproduced by a diffusion and feedback processes.

Horizontal cells, in general, form a lamina, the S-space (Naka and Rushton, 1967), and turtle horizontal cells are no exception (Simon, 1973; Saito et al., 1974). However, changes in the waveform of the response caused by changes in the size of the area illuminated have not been examined in detail. Foerster et al. (1977) showed that some cat horizontal cells produced a faster (frequency-wise) response for the stimulation of large areas, and the records of Piccolino et al. (1981) showed that the waveform of the step-evoked turtle horizontal cell responses showed a faster return to the dark level with the stimulation of a large area. The phenomenon is similar to that observed and referred to as the cutoff (Naka, 1969). With an increase in the area stimulated, turtle horizontal cells showed a faster and more differentiating response, as shown by the kernels in Fig. 13. The changes are very similar to the changes in the kernels with an increase in the mean luminance (Fig. 6). There is no possibility that rod inputs modified the dynamics, since the mean luminance we used was great enough to saturate them and the observed frequency characteristics were so rapid. The well-known feedback interactions between horizontal cells and receptors in the turtle retina (Fuortes et al., 1973; Gerschenfeld and Piccolino, 1980) are an interesting candidate for such conversions of dynamics.

We found that the presence of a steady annulus of light markedly changed the amplitude as well as the waveform of the spot-evoked kernels. This enhancement of the spot response by an annular input was rather surprising but was in accord with two other findings, namely that white-noise stimuli of brighter mean luminance produced faster kernels and that stimulation of a larger area also made the kernels faster. The three conditions that produced faster kernels had a common feature, i.e., a larger steady hyperpolarization. It may be that the assumed feedback from the horizontal cells to receptors was instrumental in the speeding up of the horizontal cell response and that the gain of the feedback was controlled by the steady hyperpolarizing level of the horizontal cells. This mechanism is consistent with the result (Appendix B) of the revised Kelly model in which the conversion of the impulse response to a more differentiating response was associated with the increase in the gain of the assumed feedback. Tranchina et al. (1984) reported evidence in turtle that supported such a feedback action to produce faster kernels. Kawasaki et al. (1984) found in catfish that the spot-evoked kernels became larger, faster, and biphasic in the presence

of a steady field (not an annulus) of light. The enhancement seen in the catfish kernels in Fig. 16*B* was produced by a steady annulus of light. Whatever the mechanism may be, the enhancement of the response dynamics by an annular or a field adapting light was seen in the horizontal cells in two very different retinas.

Naka et al. (1975) proposed that in catfish retina, a field of light produces a condition under which the horizontal cell's response becomes faster whether the response is evoked by a field or by a spot together with an (independently modulated) annular input. This was reflected in the shorter peak response time as well as in the kernel's band-pass waveform. It was proposed that the changes seen were produced by a feedback mechanism that existed between the horizontal cells and receptors, where chemical synapses, which might underlie the process, have been observed (Davis and Naka, 1980). It is also known that, under some conditions, the catfish horizontal cells increase their uptake of GABA and that its antagonist removes the proposed feedback (Lam et al., 1978). In other retinas, the external (cone) horizontal cells are known to accumulate GABA as in catfish. In this study, we have found that the dynamics of turtle horizontal cells were surprisingly similar to those found in the catfish horizontal cells. However, we have found that GABA antagonists do not alter the dynamics of the horizontal cell response in the turtle as they do in catfish.

The effects of GABA antagonists on turtle horizontal cells were the subject of earlier studies by Piccolino et al. (1982) and Gerschenfeld et al. (1982). They reported that the presence of GABA antagonists decreased the junctional communications between the large-field horizontal cells, as evidenced by both an increased coupling resistance between them and a narrowing of the receptive field. On the basis of these findings, they suggested that the results of Lam et al. (1978) might be explained by a reduced spread of current in the horizontal cell lamina similar to that observed in turtle. If so, one would expect a change in the turtle horizontal cell response dynamics similar to that observed in catfish.

We examined this possibility with bicuculline concentrations up to 100 μM, perfused for more than 30 min while recording from turtle horizontal cells, but we found that the response of the turtle horizontal cells remained unchanged (Fig. 17*A*). Correlograms from random grating experiments in these cells, however, showed a small reduction of receptive field size consistent with the findings of Piccolino et al. (1982). Consequently, the coupling resistance change may not be the mechanism involved in the conversions of dynamics to faster and more differentiating responses.

Further investigation will be needed to determine the mechanism underlying the experimental results presented in this paper. The present results reveal an important adaptive process relevant to normal visual experience under conditions of ambient illumination wherein a steady annulus of light has dramatic effects in the enhancement of response dynamics and incremental sensitivity to changes in spot luminance.

APPENDIX A

Visual sensitivity can be systematically described by separating the response into the static and dynamic parts. Steady hyperpolarization defines the absolute (or DC) sensitivity,

which is given by V_0/I_0. This sensitivity is statically nonlinear for cones and horizontal cells and can be approximated by the empirical Naka-Rushton equation (Naka and Rushton, 1966) or its modification. The local slope of the absolute sensitivity curve represents a static incremental sensitivity and has a relationship with the first-order kernel. Suppose a sudden increase in luminance, δI, is forced upon a steady mean, I_0, at $t = 0$ and the change in potential is calculable from Eq. 2*b*. The membrane potential will relax to a steady level, $V_0(I_0) + \delta I(\Delta V_0/\Delta I_0)$, after a sufficiently long time. The local slope of the absolute sensitivity curve defines the static incremental sensitivity, $\bar{S}_i$, and is expressed in terms of the first-order kernel:

$$\bar{S}_i = \frac{\Delta V_0}{\Delta I_0} = \int_0^\infty h(t; I_0)dt. \tag{5}$$

Sensitivity can also be defined to reflect a cell's response dynamics; the temporal dynamics (frequency response) of a cell depend on the mean luminance and contrast. Suppose a brief flash with an intensity I^* and a duration Δt is imposed on a (background) illumination, I_0. The perturbation with a stimulus stength $\Delta I = I^*\Delta t$ produces a small potential fluctuation that is expressed as:

$$V(t) = V_0(I_0) + \Delta I \cdot h(t; I_0). \tag{6}$$

The potential change, $\Delta V(t) = V(t) - V_0(I_0)$, generated by a criterion stimulus, ΔI, defines the dynamic incremental sensitivity, $S_i(t)$, as:

$$S_i(t) = \frac{\Delta V(t)}{\Delta I} = h(t; I_0). \tag{7}$$

This is identical to the dynamic sensitivity defined by Naka et al. (1979), which can be measured by cross-correlating the response against light stimulus. In the past, Baylor and Hodgkin (1973) also defined the step and flash sensitivities for the linear responses evoked from turtle cones in the dark, and the static and dynamic sensitivities defined in Eqs. 5 and 7 are a comprehensive extension of their sensitivities to the general case with mean luminance.

The test flash has a contrast defined as $\Delta I/I_0$, and the dynamic contrast sensitivity, $S_c(t)$, is expressed as:

$$S_c(t) = \frac{\Delta V(t)}{\Delta I/I_0} = I_0 \cdot h(t; I_0). \tag{8}$$

The contrast sensitivity can be measured by cross-correlating the response against light stimulus before it is attenuated, as shown in Fig. 1, because neutral density filters decrease the mean as well as the modulation amplitude but not contrast. The two sensitivities can be converted from one to the other if the value of neutral density filters interposed is known. Note that the two dynamic sensitivities defined by Eqs. 7 and 8 also define a cell's temporal dynamics (frequency response).

There is a simple relationship between the static and dynamic incremental sensitivities:

$$\bar{S}_i = \int_0^\infty S_i(t)dt. \tag{9}$$

The static sensitivity, $\bar{S}_i$, is defined by the local slope of the absolute DC sensitivity curve, V_0/I_0, which is approximated by the empirical Naka-Rushton equation:

$$\bar{S}_i = \frac{\sigma V_{max}}{(I_0 + \sigma)^2}, \tag{10}$$

where V_{max} is the maximum potential excursion and σ is the value of I_0 to produce $V_{max}/2$. If the response dynamics show constant-gain low-pass characteristics around a mean luminance over a large range of mean luminance, as seen in catfish horizontal cells, an incremental or decremental step-evoked response does not show any transients and the plateau of the response follows the Naka-Rushton relationship. In such a case, the dynamic incremental sensitivities, as well as the static sensitivity, can be expressed using the local slope of the Naka-Rushton relationship:

$$[S_i(t)]_{peak} = K \cdot \bar{S}_i, \tag{11}$$

where K is a constant. On the other hand, turtle horizontal cells change their dynamics from monophasic to biphasic as mean luminance increases, and, at higher mean luminance, an incremental or decremental step-evoked response shows an initial transient followed by a plateau maintained during the step input. The plateau is a reflection of the static behavior approximated by the Naka-Rushton equation, while the transient is a reflection of the biphasic characteristics of dynamics. Therefore, the dynamic incremental sensitivity of the turtle horizontal cells must deviate from the Naka-Rushton relationship, and was actually approximated by the well-known Weber-Fechner relationship as:

$$[S_i(t)]_{peak} = \frac{k}{I_0 + I_D}, \tag{12}$$

where k is a constant and I_D corresponds to the "dark light" introduced by Fechner (1966; "eigengrau" in his case) and others (Rose, 1948; Barlow, 1957; Rushton, 1962). Although both Eqs. 10 and 12 decrease monotonically with an increase in mean luminance, the former shows the steeper reduction. This is easily seen when Eqs. 10 and 12 are plotted in a log-log scale, as in Fig. 12*A*: the static incremental sensitivity (the local slope of the Naka-Rushton relationship) has an asymptotic slope of -2, while the dynamic one (the Weber-Fechner relationship) has that of -1 (the so-called Weber-Fechner slope). In other words, the static contrast sensitivity (given by $I_0\bar{S}_i$) decreases monotonically with an asymptote of -1 in a log-log scale, whereas the dynamic contrast sensitivity remains almost unchanged. The conversion from the Naka-Rushton to the Weber-Fechner relationship is a reflection of the biphasic characteristics of response, which is strengthened as mean luminance increases, probably because of a feedback action between the horizontal cells and cones (see Discussion). As a result, turtle horizontal cells show the Naka-Rushton and Weber-Fechner relationships: the former is for the static response and the latter is for the dynamic response.

APPENDIX B

The model that Kelly (1971) presented to account for the impulse responses of human visual data measured for uniform flicker illumination was composed of two stages: a diffusion process, followed by a feedback-inhibition process. The impulse responses, derived either experimentally or from his model, are remarkably similar to the first-order kernels of turtle horizontal cells in that (*a*) the amplitude became smaller, (*b*) the peak response time decreased, and (*c*) the waveform transformed in a more biphasic fashion as the mean luminance level increased. We examined his model by choosing a set of values for the model parameters and found that his original model produced a longer delay of responses than the turtle impulse response (first-order kernel). We therefore modified his model to reproduce the first-order kernels of turtle horizontal cells. The network of the revised model consists of three processes, as shown in Fig. 19: a two-stage low-pass filter, a diffusion and a feedback (inhibition) process. The dynamics of the model system are obtained by cascading the transfer functions (as functions of modulation frequency, f) of

the three processes. The first low-pass process has the transfer function, $G_1(\omega)$, at frequency $(2\pi f)$ as:

$$G_1(\omega) = \frac{1}{(1 + j\omega T)^2}. \tag{13}$$

Here j is the square root of -1 and T is a time constant chosen tentatively to be 16.7 ms. The diffusion process has the following assumptions: (*a*) a photoinduced signal is carried by a substance that diffuses one-dimensionally from $x = 0$ to $x = \xi$; (*b*) the concentration of the substance satisfies a diffusion equation with a diffusion constant D and a rate constant ρ of inactivation (leak and/or binding of the diffusing substance); (*c*) the inactivation occurs at $x = \infty$ (even if it is made $x = \xi$, similar results are obtained); (*d*) the signal transfer is determined by the ratio of the flux of the diffusing substance at $x = \xi$ and that at $x = 0$. Kelly ignored the inactivation in his computation, but we retained it. Therefore, the transfer function, $G_d(\omega)$, of the diffusion process is expressed as (Kelly, 1971):

$$G_d(\omega) = C \cdot \exp\left[-\sqrt{2\tau(\rho + j\omega)}\right], \tag{14}$$

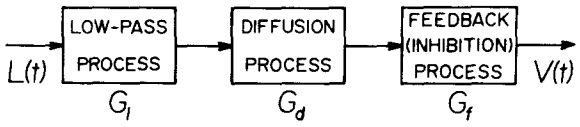

FIGURE 19. A schematic representation of the model network, which consists of three processes. $L(t)$ is the photic stimulus and $V(t)$ is the response from a horizontal cell. The transfer function of each process is given in Eqs. 13, 14, and 15.

where $\tau = \xi/2D$ and C is a constant. At the final stage of the feedback process, the amplitude of the lower-frequency component is attenuated. For this stage, we used the same transfer function, $G_f(\omega)$, that Kelly proposed as an extension of the closed-loop transfer function of a circuit having a simple feedback loop (Kelly, 1971):

$$G_f(\omega) = \left[\frac{(j\omega + \alpha)^2}{(j\omega + K)^2 + K^2}\right]^{r/2}. \tag{15}$$

Here K corresponds mainly to the gain of feedback, α represents the time constant of integrators within the network, and r is related to the multiplicity of internal feedback loop. The model system shows piecewise linear dynamics around the mean luminance level if all the parameters incorporated in the model are fixed, depending upon the mean level. We assume that the parameters C, ρ, K, α, and r vary with mean luminance level, and the values of parameters are determined to fit the experimental result. To do this, the first-order kernels at each mean luminance in Fig. 7 were averaged, and the averaged kernel was Fourier-transformed by an FFT algorithm and the amplitude (gain) of the transfer function was computed. The parameters τ, C, and ρ of the diffusion process were first determined to fit the high-frequency asymptotes (above roll-off frequency) of the experimental transfer function thus obtained, and then the luminance-invariant parameter τ was determined to be 0.5 s. The parameters K, α, and r of the feedback process were next determined to fit the lower-frequency part (below roll-off frequency) of the amplitude of the transfer function, and then the value of r was 4, which shows its independence of mean luminance (and, therefore, the unchained structure of the network). The remaining

TABLE I

Values of Parameters Incorporated in the Model of Fig. 19

	Diffusion process		Feedback process	
Attenuation	C	ρ	$K/2\pi$	$\alpha/2\pi$
		s^{-1}	*Hz*	*Hz*
0 log	1	20	7.0	5.0
1 log	2.6	3.0	6.7	3.2
2 log	3.6	1.0	5.4	3.3
3 log	7.2	0.1	3.7	3.1

The parameter C is given by the ratio to the value of 0 log luminance level. For the remaining parameters, see text.

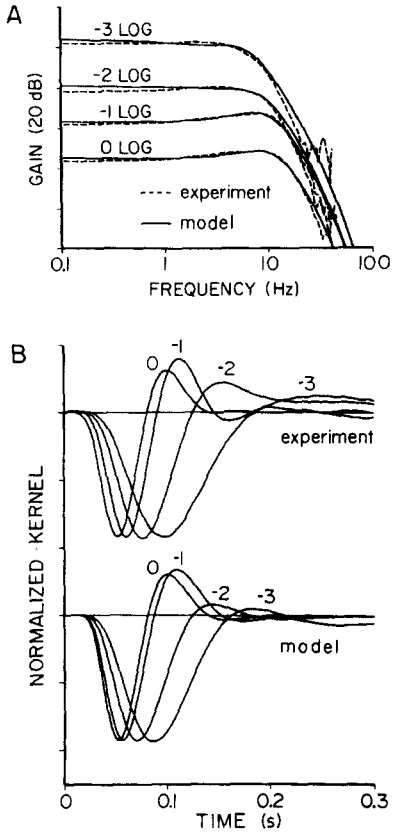

FIGURE 20. Gain functions (*A*) and first-order kernels (*B*) computed by averaging the experimental data and from the modified Kelly model. An average of the first-order kernels at each mean luminance produced the experimental kernel (in *B*), which was Fourier-transformed to give the experimental gain function (dotted line in *A*). A set of model gain functions (solid line in *A*) based on the modified Kelly model was determined to fit the experimental gain functions and inversely Fourier-transformed to produce a set of model kernels (in *B*).

values of the parameters are shown in Table I, in which both the rate, ρ, of inactivation and the gain, K, of feedback increase with an increase in mean luminance. In particular, the change of impulse response from monophasic to biphasic is due to the increase of feedback magnitude (K), which decreases the gain of the overall system at the lower frequency. Using these values, the model transfer function was computed by multiplying the transfer functions of three stages, and the model impulse responses were computed by an inverse FFT algorithm from the model transfer functions. Fig. 20 shows the transfer functions (gains only) and first-order kernels, averaged and modeled. Thus, the modified Kelly model reproduced very well the observed first-order kernels.

We thank Yu-ichiro Ando for his programming assistance.
This research was partly supported by National Institutes of Health grants EY-00777 and EY-01897.

Original version received 9 July 1984 and accepted version received 21 May 1985.

REFERENCES

Barlow, H. B. 1957. Incremental thresholds at low intensities considered as signal/noise discriminations. *J. Physiol. (Lond.)*. 136:469–488.

Baylor, D. A., and A. L. Hodgkin. 1973. Detection and resolution of visual stimuli by turtle photoreceptors. *J. Physiol. (Lond.)*. 234:163–198.

Burkhardt, D. A. 1974. Sensitization and centre-surround antagonism in *Necturus* retina. *J. Physiol. (Lond.)*. 236:593–610.

Cervetto, L., and E. F. MacNichol, Jr. 1972. Inactivation of horizontal cells in turtle retina by glutamate and aspartate. *Science (Wash. DC)*. 178:767–768.

Davis, G. W., and K.-I. Naka. 1980. Spatial organization of catfish retinal neurons. I. Single- and random-bar stimulation. *J. Neurophysiol. (Bethesda)*. 43:807–831.

Fechner, G. T. 1860. Elementa der psychophysik. Breitkopf und Härtel, Leipzig. *In translation*: 1966. Elements of Psycophysics. H. E. Adler, D. H. Howes, and E. G. Boring, editors. Holt, Rinehart and Winston, Inc., New York. 286 pp.

Foerster, M. H., W. A. van de Grind, and O.-J. Grusser. 1977. The response of cat horizontal cells to flicker stimuli of different area, intensity and frequency. *Exp. Brain Res.* 29:367–385.

Fuortes, M. G. F., E. A. Schwartz, and E. J. Simon. 1973. Colour dependence of cone responses in turtle retina. *J. Physiol. (Lond.)*. 234:199–216.

Gerschenfeld, H. M., J. Neyton, M. Piccolino, and P. Witkovsky. 1982. L-horizontal cells of turtle: network organization and coupling modulation. *Biomed. Res.* 3(Suppl.):21–34.

Gerschenfeld, M., and M. P. Piccolino. 1980. Sustained feedback effects of L-horizontal cells on turtle cones. *Proc. R. Soc. Lond. B Biol. Sci.* 206:465–480.

Kawasaki, M., K. Aoki, and K.-I. Naka. 1984. Effects of background and spatial patterns on incremental sensitivity of catfish horizontal cells. *Vision Res.* 24:1197–1204.

Kelly, D. H. 1971. Theory of flicker and transient responses. I. Uniform fields. *J. Opt. Soc. Am.* 61:537–546.

Lam, D. M.-K., E. M. Lasater, and K.-I. Naka. 1978. Gamma aminobutyric acid: a neurotransmitter candidate for cone horizontal cells of the catfish retina. *Proc. Natl. Acad. Sci. USA.* 75:6310–6313.

Leeper, H. F. 1978. Horizontal cells of the turtle retina. I. Light microscopy of Golgi preparations. *J. Comp. Physiol.* 182:777–794.

Marmarelis, P. Z., and K.-I. Naka. 1972. White-noise analysis of a neuron chain: an application of the Wiener theory. *Science (Wash. DC)*. 175:1276–1278.

Marmarelis, P. Z., and K.-I. Naka. 1973. Nonlinear analysis and synthesis of receptive-field responses in the catfish retina. III. Two-input white-noise analysis. *J. Neurophysiol. (Bethesda)*. 36:634–648.

McKean, H. P. 1973. Wiener's theory of nonlinear noise. *In* Stochastic Differential Equations. J. S. Keller and H. P. McKean, editors. *SIAM-AMS Proc.* 6:191–209.

Naka, K.-I. 1969. Factors influencing the time course of S-potentials. *J. Physiol. (Lond.)*. 200:373–385.

Naka, K.-I., R. Y. Chan, and S. Yasui. 1979. Adaptation in catfish retina. *J. Neurophysiol. (Bethesda)*. 42:441–454.

Naka, K.-I., P. Z. Marmarelis, and R. Y. Chan. 1975. Morphological and functional identifications of catfish retinal neurons. III. Functional identification. *J. Neurophysiol. (Bethesda)*. 38:92–131.

Naka, K.-I., and W. A. H. Rushton. 1966. S-potentials from colour units in the retina of fish (*Cyprinidae*). *J. Physiol. (Lond.)*. 185:536–555.

Naka, K.-I., and W. A. H. Rushton. 1967. The generation of S-potentials in fish (*Cyprinidae*). *J. Physiol. (Lond.)*. 192:437–461.

Naka, K.-I., M. Sakuranaga, and R. L. Chappell. 1982. Wiener analysis of turtle horizontal cells. *Biomed. Res.* 3(Suppl.):131–136.

Piccolino, M., J. Neyton, and H. Gerschenfeld. 1981. Center-surround antagonistic organization in small-field luminosity horizontal cells of the turtle retina. *J. Neurophysiol. (Bethesda)*. 45:363–375.

Piccolino, M., J. Neyton, P. Witkovsky, and H. M. Gerschenfeld. 1982. γ-Aminobutyric acid antagonists decrease junctional communication between L-horizontal cells of the retina. *Proc. Natl. Acad. Sci. USA*. 79:3671–3675.

Rose, A. 1948. The sensitivity performance of the human eye on an absolute scale. *J. Opt. Soc. Am.* 38:196–208.

Rushton, W. A. H. 1965. The Ferrier Lecture, 1962: Visual adaptation. *Proc. R. Soc. Lond. B Biol. Sci.* 162:20–46.

Saito, T., W. H. Miller, and T. Tomita. 1974. C- and L-type horizontal cells in the turtle retina. *Vision Res.* 14:119–123.

Sakuranaga, M., and K.-I. Naka. 1985. Signal transmission in the catfish retina. I. Transmission in the outer retina. *J. Neurophysiol. (Bethesda)*. 53:373–389.

Simon, E. J. 1973. Two types of luminosity horizontal cells in the retina of the turtle. *J. Physiol. (Lond.)*. 230:199–211.

Tranchina, D. 1981. Systems analysis of the spatial and temporal properties of horizontal cells in the turtle retina. PhD. Dissertation. The Rockefeller University, New York.

Tranchina, D., J. Gordon, and R. Shapley. 1983. Spatial and temporal properties of luminosity horizontal cells in the turtle retina. *J. Gen. Physiol.* 82:573–598.

Tranchina, D., J. Gordon, and R. Shapley. 1984. Retinal light adaptation—evidence for a feedback mechanism. *Nature (Lond.)*. 310:314–316.

Tranchina, D., J. Gordon, R. Shapley, and J.-I. Toyoda. 1981. Linear information processing in the retina: a study of horizontal cell responses. *Proc. Natl. Acad. Sci. USA*. 78:6540–6542.